Icarus 000 (2016) 1–9

Contents lists available at ScienceDirect

Icarus

journal homepage: www.elsevier.com/locate/icarus

The structural stability of lunar lava tubes

David M. Blair[a,1,*], Loic Chappaz[b], Rohan Sood[b], Colleen Milbury[a], Antonio Bobet[c], H. Jay Melosh[a,d], Kathleen C. Howell[b], Andrew M. Freed[a]

[a] Department of Earth, Atmospheric, and Planetary Sciences, Purdue University, 550 Stadium Mall Dr., West Lafayette, IN 47907, USA
[b] School of Aeronautics and Astronautics, Purdue University, 701 W. Stadium Ave., West Lafayette, IN 47907, USA
[c] Lyles School of Civil Engineering, Purdue University, 550 Stadium Mall Dr., West Lafayette, IN, 47907, USA
[d] Department of Physics and Astronomy, Purdue University, 525 Northwestern Ave., West Lafayette, IN 47907, USA

ARTICLE INFO

Article history:
Available online xxx

Keywords:
Moon
Lava tube, volcanism
Skylight (hole)
GRAIL

ABSTRACT

Mounting evidence from the SELENE, LRO, and GRAIL spacecraft suggests the presence of vacant lava tubes under the surface of the Moon. GRAIL evidence, in particular, suggests that some may be more than a kilometer in width. Such large sublunarean structures would be of great benefit to future human exploration of the Moon, providing shelter from the harsh environment at the surface—but could empty lava tubes of this size be stable under lunar conditions? And what is the largest size at which they could remain structurally sound? We address these questions by creating elasto-plastic finite element models of lava tubes using the Abaqus modeling software and examining where there is local material failure in the tube's roof. We assess the strength of the rock body using the Geological Strength Index method with values appropriate to the Moon, assign it a basaltic density derived from a modern re-analysis of lunar samples, and assume a 3:1 width-to-height ratio for the lava tube. Our results show that the stability of a lava tube depends on its width, its roof thickness, and whether the rock comprising the structure begins in a lithostatic or Poisson stress state. With a roof 2 m thick, lava tubes a kilometer or more in width can remain stable, supporting inferences from GRAIL observations. The theoretical maximum size of a lunar lava tube depends on a variety of factors, but given sufficient burial depth (500 m) and an initial lithostatic stress state, our results show that lava tubes up to 5 km wide may be able to remain structurally stable.

1. Introduction

Lunar lava tubes present an enticing target for future human lunar exploration. A vacant lava tube could provide astronauts shelter against small meteorite impacts, cosmic radiation, and the extreme temperature variations at the lunar surface (Hörz, 1985; Haruyama et al., 2012). Because lava tubes are by their nature found in the vicinity of volcanic vents, there may also be good local availability of volatile chemical species such as sulfur, iron, and oxygen, as well as pyroclastic debris which could be useful as a construction material (Coombs and Hawke, 1992). Their enclosed nature and limited exposure to the space environment may also make them possible storage locations for water and other ice deposits, useful sites for studying the stratigraphy of the lunar regolith and dust environment, and suitable sites for finding comparatively pristine examples of mantle-derived rocks near the surface (Haruyama et al., 2012). Locating and characterizing potential lunar lava tubes has therefore been a priority in the lunar science community for some time.

Lava tubes form when a channelized lava flow forms a roof either through the development of levees or the formation of a surficial crust, while the molten material underneath flows away and leaves a partially or completely vacant conduit (e.g. Cruikshank and Wood, 1971). Such features occur in numerous locations on Earth, and it has long been posited that they may also exist—or have existed—on the Moon. Through interpretation of images returned by Lunar Orbiter V, Oberbeck et al. (1969) were among the first to suggest that sinuous rilles such as those observed in northern Oceanus Procellarum and elsewhere may be the collapsed remains of lava tubes which formed during the emplacement of the maria. Numerous other studies during the Lunar Orbiter and Apollo mission eras supported this idea, and showed examples of similar processes occurring in Hawai'i (e.g. Cruikshank and Wood, 1971; Greeley, 1971; Oberbeck et al., 1972).

It is only recently that we have obtained direct evidence for the existence of uncollapsed voids beneath the lunar surface. In 2009, Haruyama et al. published their discovery of a 65 m-diameter

* Corresponding author.
E-mail address: david_blair@brown.edu (D.M. Blair).
[1] Present address: Department of Earth, Environmental, and Planetary Sciences, Brown University, Box 1846, 324 Brook St., Providence, RI 02912, USA.

http://dx.doi.org/10.1016/j.icarus.2016.10.008
0019-1035/

vertical-walled hole in the Marius Hills region of the Moon, using data from the Terrain Camera and Multi-band Imager aboard the SElenological and ENgineering Explorer (SELENE) spacecraft. The following year, two additional pits were identified in SELENE data, in Mare Tranquilitatis and Mare Ingenii (Haruyama et al., 2010). Subsequent high-resolution imagery returned by the Lunar Reconnaissance Orbiter Camera (LRO/LROC) (Robinson et al., 2010) was then used not only to provide more detailed views of the pits discovered by Haruyama et al. (2009, 2010), but also to identify 150 additional pits at the lunar surface (Robinson et al., 2012). Overall, these openings are found to have widths ranging from 49 to 106 m, which represents a minimum size for the underlying void, and oblique views of the pits do show that the underlying cavern is wider than the hole in the surface in at least several cases (Ashley et al., 2011; Wagner and Robinson, 2014). Voids may also exist in areas such as the Al-Tusi impact melt pond near King Crater on the lunar far side, where skylights and sinuous fracture patterns have been found in high-resolution LROC images (Ashley et al., 2012), suggesting a lava tube collapse. Unfortunately, the size and shape of a void cannot be determined by the use of imagery alone (e.g. Robinson et al., 2012).

Gravity data, however, is particularly suited to the identification and characterization of subsurface density variations such as vacant lava tubes. Work by Chappaz et al. (2014a,b, 2016) and Sood et al. (2016a,b) has shown that lava tubes, buried craters, and other density anomalies can be located and characterized in the high-resolution datasets returned by NASA's Gravity Recovery And Interior Laboratory (GRAIL) mission (e.g. Zuber et al., 2013; Lemoine et al., 2014). Using a combination of techniques such as gravity anomaly Eigenvalue mapping, cross-correlation between observed gravity signals and those of hypothetical features, and forward modeling of the gravity anomalies caused by lava tubes, Chappaz et al. (2014a,b, 2016) have found possible sublunarean extensions of surface sinuous rilles at both Vallis Schröteri and Rima Sharp. In both cases, GRAIL observations were found to positively correlate with a buried tube 1–2 km in width. The depth and shape of these putative lava tubes cannot be explicitly determined from gravity data, however, as a tube even several hundred meters under the surface would produce a nearly identical GRAIL-observable gravity signature to one sitting centimeters under the surface since in both cases the spacecraft's altitude would be much greater than the feature's depth. While a collection of smaller lava tubes could also produce a gravity signature that would match GRAIL observations, the general pattern of volcanic flows on the Moon is one characterized by a relatively small number of high-volume flows. The interpretation favored here and in Chappaz et al. (2014a,b, 2016) and Sood et al. (2016a), therefore, is that these gravity anomalies are each caused by a single, large vacant lava tube buried at some non-zero distance under the surface.

The size of the lava tubes inferred by Chappaz et al. (2014a,b, 2016) is much larger than any known terrestrial examples, which reach a maximum of ~30 m in width (e.g. Greeley, 1971). Oberbeck et al. (1969) addressed the question of how large a lava tube could be on the Moon and remain structurally stable by modeling the roof of a lava tube as an elastic beam. Doing so, they found that a lava tube with a roof 65 m thick could remain stable at a width of $\lesssim$ 385 m, given a lunar basalt density of 2500 kg m^{-3}. They also suggest that lava tubes up to 500 m wide may be possible under lunar conditions, a number which has been frequently cited since that work was published; that calculation, however, uses a hypothetical vesicular basalt density of 1500 kg m^{-3}, well below the 3010–3270 kg m^{-3} density of that material which is now known from modern re-analysis of Apollo mare samples (Kiefer et al., 2012). Furthermore, while Oberbeck et al. (1969) mention that an arched roof would allow a larger stable tube or a thinner possible roof at a given tube width than the beam model used in their study, they do not quantify that effect.

In this study, we aim to constrain the maximum size at which vacant lava tubes could remain structurally stable under lunar gravity. More specifically, we seek to determine whether the large lava tubes inferred from analysis of GRAIL data by Chappaz et al. (2014a,b, 2016) are mechanically plausible, leaving aside the mechanisms for forming tubes of that scale. Our methods incorporate numerical modeling techniques of a scale not available to investigations of similar questions performed during the Apollo era, as well as modern knowledge about the densities of lunar rocks and the behavior and failure mechanisms of large rock bodies in general.

2. Modeling techniques

We approach the question of lava tube stability through the use of finite element models built in the *Abaqus* software suite (version 6.12; http://www.simulia.com/solutions). Our models assume plane-strain conditions and are symmetric about the tube's longitudinal axis for the sake of computational simplicity. Models were verified against analytic results for simple cases (e.g. gravitational self-compression of a block) and were found to be accurate to within 1%. Zero-motion boundary conditions are set at the far lateral and bottom edges of the model, which are placed sufficiently far away (20 tube widths) so as not to influence our model results. In every model, we ensure that there are 20 elements through the thickness of the lava tube's roof, and then adjust other mesh parameters to ensure suitable element aspect ratios ($<$ 10:1). Our general model setup and an example mesh are shown in Fig. 1. We do not model the formation of the lava tube itself, but instead investigate the stability of the completed structure under various potential lunar conditions.

The primary variables in this study are the width of the lava tube, the thickness of the lava tube's roof, and the pre-existing stress state of the material. The shape of the tubes is held at a constant 3:1 width-to-height ratio, mimicking the general non-circular arched shape of terrestrial lava tubes while remaining somewhat close to the circular cross-section used in Chappaz et al. (2014a,b, 2016) such that our models do not grossly over-predict the width of the tube responsible for a particular gravity deficit. The fixed aspect ratio also means that we are varying the tube's volume linearly by adjusting only the width, which is useful for comparison with analyses of GRAIL data since these scales with the volume of the void space. While this single aspect ratio cannot represent the various lava tube shapes on the Moon or elsewhere, focusing on a single shape also enables efficient exploration of parameter space in terms of width, roof thickness, and initial stress state (see next paragraph). Because these structures are buried, the roof thickness is in one sense equivalent to the depth to which a lava tube has been buried by one or more flows after its initial formation. It can also be considered as the thickness of the thinnest layer within the lava tube's roof, however, by analogy to terrestrial caves in bedded rock which tend to collapse when individual beds start to fail (e.g. Ford and Williams, 1994; Palmer, 2007). We therefore test a range of roof thickness values from 1 to 500 m that includes both the range of layer thicknesses seen in the walls of lunar skylights (~1–12 m) (Robinson et al., 2012) and a thickness comparable to the larger flows in Oceanus Procellarum (~600 m) (Wieder et al., 2010). Our modeled lava tube widths range from 250 m to 10 km, representing a size slightly smaller than the maximum size calculated by Oberbeck et al. (1969) and the approximate present-day width of the widest part of Vallis Schröteri, respectively. With our assumed width-to-height ratio, this range also includes lava tubes with heights similar to the ~100–150 m depths of observed skylights.

Please cite this article as: D.M. Blair et al., The structural stability of lunar lava tubes, Icarus (2016), http://dx.doi.org/10.1016/j.icarus.2016.10.008

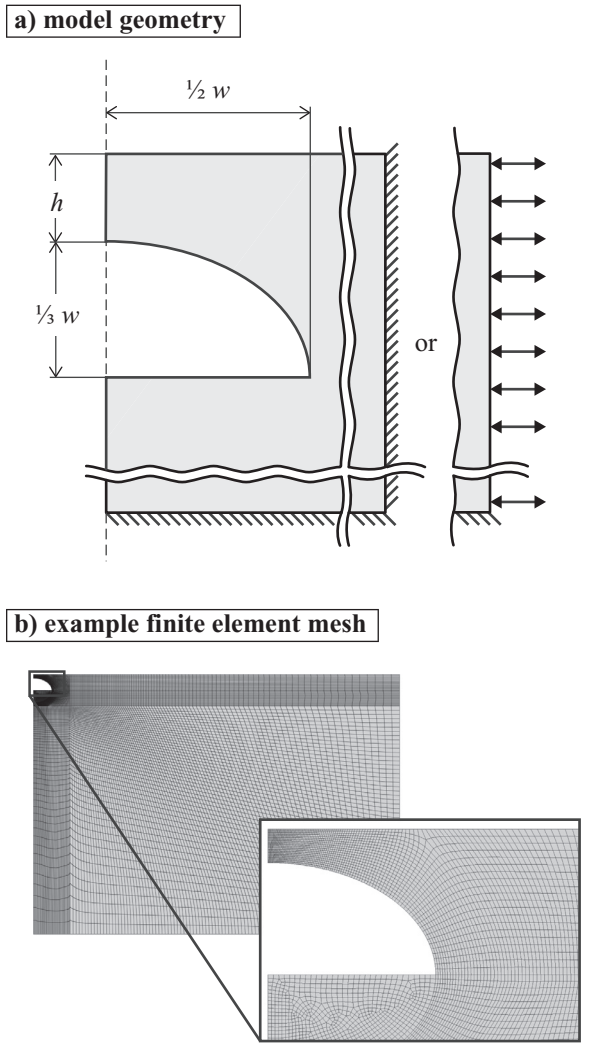

Fig. 1. (a) Diagram of our model configuration showing our geometric variables: the lava tube's width, *w*, and the thickness of its roof, *h*. The height of the lava tube is set at ⅓ of its total width. Our model is symmetric about a plane bisecting the lava tube lengthwise (dashed line), and extends infinitely into and out of the page due to our assumption of plane-strain conditions. The right and bottom edges of the model are 20 *w* away from the plane of symmetry and the surface of the model, respectively, and the bottom of the model is fixed. The right edge of the model is either fixed or set to a given horizontal displacement, depending on whether or not the model includes far-field tectonic strains. (b) Example finite element model mesh, and an inset showing details of the mesh in the region of the lava tube.

We simulate lava tubes which have formed in either a lithostatic or Poisson stress state, representing two end-member cases of how stresses in the emplaced and cooled lava could be distributed. The lithostatic stress state is one where the horizontal stresses at depth are equal to the overburden (vertical) stress, a state which would arise if all of the materials comprising the lava tube and its surroundings were able to relax differential stresses completely after emplacement; in geotechnical engineering terms, the lithostatic state is defined as one where the coefficient of earth pressure at rest, k_0, is equal to unity. The Poisson stress state represents the material's direct elastic response to overburden, where horizontal stresses at depth are some fraction (usually on the order of ⅓, given a typical basaltic Poisson ratio of 0.25 as used here; see Table 1) of the vertical stress and are controlled by the material's Poisson ratio. To obtain our results for the Poisson stress state, we simply allow the structure to self-compress under lunar gravity with zero-horizontal-motion (and free vertical motion) boundary conditions at the lateral edges of the model. This is the only model run necessary to initiate a Poisson stress state. In contrast, the development of an initial lithostatic stress state requires an iterative process that balances gravity loads with applied stresses such that no significant gravitational self-compression occurs in regions far from the lava tube. We accomplish this by running a version of the self-compression simulation that only includes elastic material properties, retrieving only the final vertical stresses from each element in the model, and assigning that vertical stress value to all three Cartesian stress components for that element in a second elastic simulation in which the elements again start at their original, undeformed positions. After running this second simulation, we typically still observe some far-field motion in the model, and so we repeat the process until far-field displacements vary by less than 1% between two successive models, typically through the 3rd or 4th iteration.

Table 1
Model parameters.

Symbol	Description	Value	Units
ρ_b	Density[a]	3100	kg m^{-3}
ν	Poisson's ratio	0.25	
σ_{ci}	Unconfined compressive strength	100	MPa
m_i	Material constant[b]	20	
GSI	Geological Strength Index[b]	70	
φ	Friction angle[c]	43	°
Ψ	Dilation angle	29	°
E	Young's modulus[c]	30	GPa
c	Cohesive strength	7.2	MPa
g_{Moon}	Lunar gravity	1.662	m s^{-2}

[a] after Kiefer et al. (2012);
[b] value from Marinos and Hoek (2000);
[c] calculated using method described in Marinos and Hoek (2000).

We also consider regional-scale tectonic strains that may affect the stability of a lava tube. To simulate these strains, we modify our models so that the edge farthest from the plane of symmetry is forced to move laterally during the simulation by an assigned percentage of the total width of the model (not of the lava tube) which varies between model runs. Edge motion towards the plane of symmetry places the model into contraction, simulating the flexural compression and subsidence associated with the emplacement of the mare which may have led to the formation of features like mare ridges. Edge motion away from the plane of symmetry places the region into extension, which might be expected if the region is undergoing flexural uplift. We vary the magnitude and sign of the tectonic strains to examine the effects of various amounts and types of tectonic deformation, since the regional strain conditions of the lunar maria are poorly constrained. These tectonic strains are superimposed onto the gravity loading described above.

The material comprising our model is assigned a Mohr–Coulomb plastic failure envelope in order to simulate stresses and strains in a way that incorporates rock failure. The parameters for the material's plasticity are chosen to represent a slightly fractured rock body as opposed to a pristine sample of intact rock so as to make our results both more realistic and more conservative, as fractures (e.g. due to cooling; see Discussion) are likely present and would make the rock body weaker than intact rock. We do this using the Geological Strength Index (GSI) method of Marinos and Hoek (2000), choosing parameter ranges appropriate to lunar basalts and then choosing the weakest values where a range is given; we assume that the rock mass forming the lava tube and its surroundings has an unconfined compressive strength σ_{ci} of 100 MPa (from a 100 to 250 MPa range given for basalt, and equivalent to sandstone), a material constant m_i of 20 (from a typical basaltic m_i range of 25 ± 5), and a GSI value of 70 (corresponding to "blocky" rock structure and zero aqueous weather-

Please cite this article as: D.M. Blair et al., The structural stability of lunar lava tubes, Icarus (2016), http://dx.doi.org/10.1016/j.icarus.2016.10.008

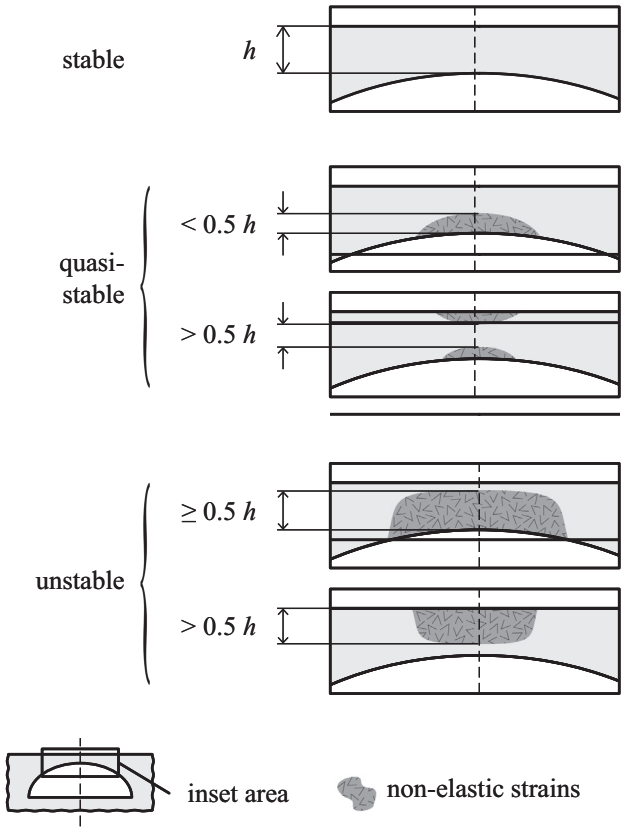

Fig. 2. Model outcome designations. We deem a tube "stable" (top) when there are no non-elastic strains in the lava tube's roof; "quasi-stable" when there are non-elastic strains in less than half of the roof's total thickness (middle); and "unstable" when non-elastic strains are present in more than half of the roof's thickness (bottom). In the latter two cases, we do not distinguish based on the location of the non-elastic strains, instead considering only their total prevalence in the roof. Illustration roughly to scale.

ing). From these, we calculate a friction angle φ of 43°, a dilation angle ψ of 29°, a deformation (Young's) modulus E of ~30 GPa, and a cohesive strength c of 7.2 MPa, using the method outlined in Marinos and Hoek (2000). In addition, we assume a basalt density of 3100 kg m^{-3}, a rough median value of the basalt densities found in a recent re-analysis of lunar samples by Kiefer et al. (2012). All of our material parameters are summarized in Table 1. This is a "continuum" approach to modeling the material, where the influence of individual fractures is ignored in favor of distributed plastic (e.g. cataclastic) deformation; this assumption becomes less reasonable with thinner lava tube roofs, as structurally critical areas represent a larger portion of the model, meaning that randomly distributed unmodeled fractures are more likely to exist in critical areas (e.g. through the apex of the roof). Nevertheless, in absence of such fractures, this approximation of the material behavior is substantially more realistic for our purposes than assuming that the rock behaves elastically.

We infer the structural stability or failure of a lava tube by calculating what proportion of the thickness of the lava tube's roof has exceeded the Mohr-Coulomb failure envelope at the end of our model simulation (Fig. 2). The rationale for this approach lies in the observed tendency of terrestrial caves to fail at the apex of the roof, progressing upwards layer by layer as the cave fails (e.g. Ford and Williams, 1994; Palmer, 2007); as stated previously, our roof thicknesses can thus be thought of as representing either the thickness of the thinnest layer in the roof or the thickness of a single but more voluminous volcanic deposit. Any amount of plastic strain in our model output is taken to indicate complete local material failure; we are not claiming that the rock body undergoes gross plastic deformation, only that it has ceased to behave elastically and is therefore likely to fail. If there are no plastic strains in the lava tube's roof, we deem the tube stable. If plastic deformation (either contractional or extensional) is present in less than 50% of the total thickness of the lava tube's roof, the structure is considered 'quasi-stable'; this could represent either the failure of several layers within the roof, or the failure of some portion of a single-layer roof. Finally, if our model indicates plastic strains in the majority (50% or more) of the roof's thickness, we conclude that this lava tube would be unstable under lunar conditions. In the latter two cases, we do not distinguish based on the location of failure zones at either the top or bottom of the roof, and instead examine the total thickness that they occupy. The choice of a cut-off point of 50% of the roof thickness is arbitrary, but having two distinct degrees of failure allows us to note both lava tubes that are beginning to fail and those in which total roof failure is more likely.

3. Results

We find that the maximum size of a stable or quasi-stable empty lunar lava tube depends strongly on both the thickness of the tube's roof and the assumed pre-existing stress state (Fig. 3). Without considering the effects of regional tectonics, our results indicate that a lava tube buried 50 m under the lunar surface can remain fully stable at a width of up to 3.5 km; if some portion of the roof is allowed to fail as in our "quasi-stable" results, both pre-existing stress state cases allow a tube 5.25 km across with a roof 200 m thick. This means that regardless of the gravitational stress state assumed to exist in the structure or the degree of local failure which is permitted (i.e. none in the stable outcomes or < 50% in the quasi-stable outcomes), our results support the interpretation of Chappaz et al. (2014a,b, 2016) that GRAIL gravity observations may represent very large vacant sublunarean lava tubes, although the question of initially forming a lava tube of this scale is a separate matter (see the Discussion). The largest possible stable or quasi-stable lava tube changes depending on our stress state assumptions, however, as does the relationship between lava tube roof thickness and stability. These differences are discussed in more detail below, along with the results of our models testing the influence of far-field tectonic strains and the cooling of the lava tube.

Assuming a lithostatic state of stress in the material, the maximum size of a stable lava tube increases with the thickness of the roof (Fig. 3, top). With our maximum tested roof thickness of 500 m, a lava tube as large as 5 km across (Fig. 4) experiences no plastic strains under lunar conditions, and lava tubes up to 6.75 km across may remain stable if they are able to survive failure occurring in a portion of the roof's thickness. Lava tubes 1 km wide as inferred from GRAIL data (Chappaz et al., 2014a,b; 2016) can remain stable given a roof at least 1 m thick, given our material assumptions and the modeled roof shape. In all cases, a lithostatic stress state leads to stresses in the roof of the lava tube that are compressional throughout its thickness (e.g. Fig. 5, color contours) similar to the designed behavior of masonry keystone arches, and when failure occurs it does so in absolute contraction (i.e. with negative lateral plastic strains) progressing from the surface of the lava tube downwards.

Lava tubes beginning in a Poisson stress state cannot remain stable at sizes quite as large as those in an initial lithostatic stress state, and the relationship between roof thickness and tube stability is more complex (Fig. 3, bottom). The largest fully stable tube in this case is found to be 3.5 km across, with a 50–100 m thick roof (e.g. Fig. 5, model D); if some plastic failure is allowed, that maximum size increases to 5.25 km with a roof thickness of 200–500 m.

Please cite this article as: D.M. Blair et al., The structural stability of lunar lava tubes, Icarus (2016), http://dx.doi.org/10.1016/j.icarus.2016.10.008

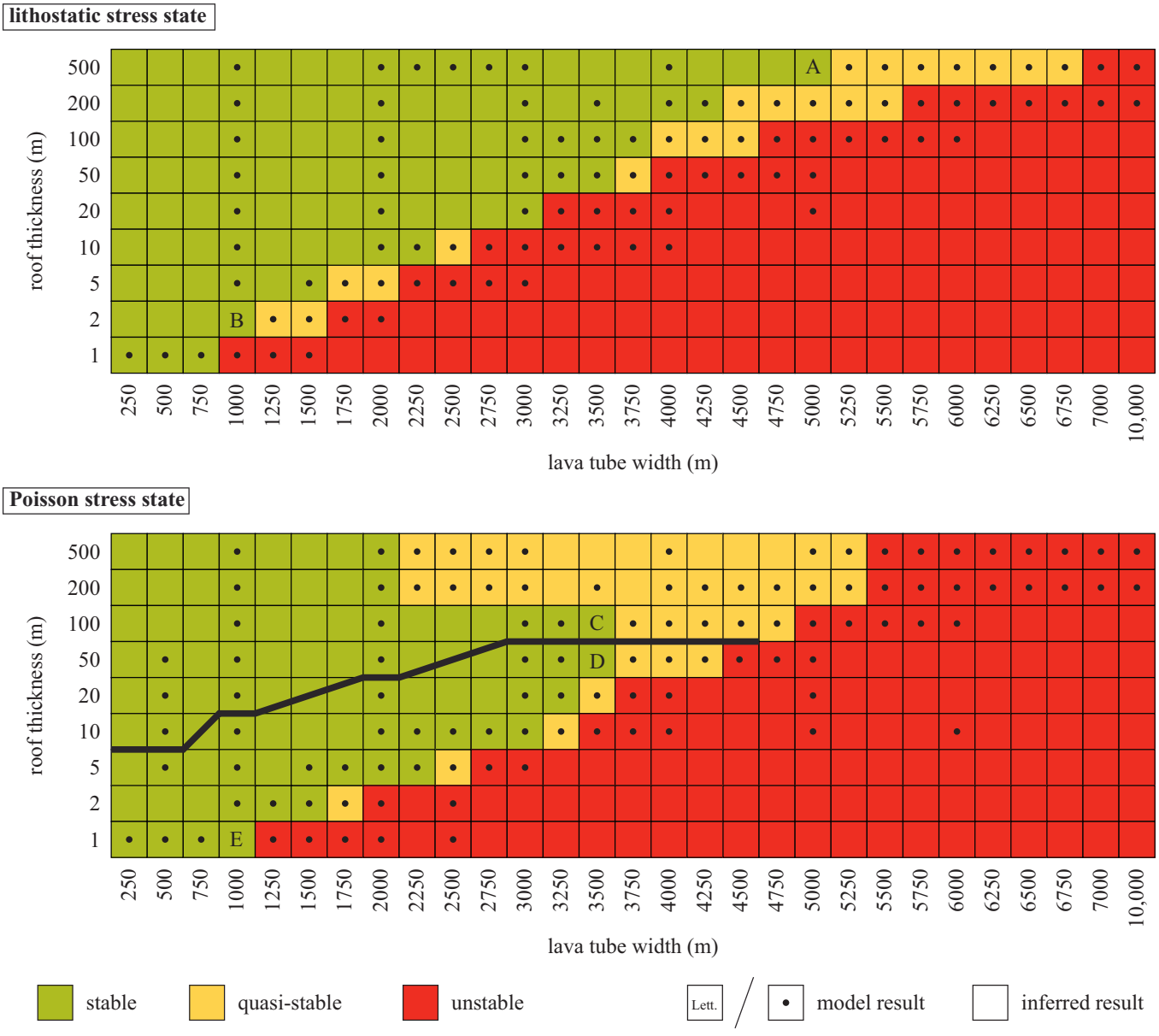

Fig. 3. Lava tube stability results from this study for an assumed lithostatic (top) and Poisson (bottom) state of stress in the material comprising the lava tube and its surroundings, and for a variety of combinations of lava tube width and roof thickness (with height fixed at ⅓ of the width). A lava tube is deemed stable when there are no plastic strains present in the roof, quasi-stable when plastic strains are present in $<50\%$ of the roof's thickness, and unstable when plastic strains are found over $\geq 50\%$ of the roof's thickness. The bold line in (b) indicates a division between two modes of failure in the Poisson models, with models below that line (and all models in the lithostatic stress state case) failing in contraction, and models above that line failing in extension due to downwards flexure of the roof. See the text for more details. Dots or letters indicate performed simulations, blank boxes indicate interpolated results; the letters correspond to models shown in Figs. 4–6.

We also find that tubes 1 km wide or wider can remain stable even with a roof thickness of only 1 m given an initial Poisson stress state and our assumptions regarding the material properties of the rock (i.e the GSI parameters and density as described in the Modeling Techniques section). However, unlike the lithostatic stress state, increasing roof thickness does not uniformly lead to larger possible tube sizes. Below a certain thickness (below the bold line in Fig. 3), the roof is entirely in compression (Fig. 5, model E), leading failure to occur in compression and at the surface, as is the case with our lithostatic stress state models. In thicker-roofed tubes (above the bold line in Fig. 3), however, the tendency of the roof to flex downwards under its own weight, combined with the lower horizontal stresses present in this stress state compared to the lithostatic stress state, leads to extension at the base of the roof (Fig. 5, model D). As rock is much weaker in tension/extension than in compression, this causes local material failure at the base of the roof, similar to the failure pattern observed in terrestrial caves in bedded deposits. The presence of this second failure mode leads to both smaller possible lava tube sizes and the observed nonlinear relationship between roof thickness and lava tube stability in our models with an initial Poisson stress state.

The failure mode of a given lava tube also affects its ability to withstand far-field tectonic strains. Fig. 6 shows a selection of models under both the lithostatic and Poisson stress states which were subjected to both contractional and extensional far-field strains (shown on the horizontal axis) until the point of failure; failure states are the same as in Fig. 3. Models that fail in contraction with no imposed far-field strains (e.g. models A, B, D, and E in Fig. 6) can be subjected to comparatively large amounts of extensional strain before failing. A small amount of imposed far-field

Please cite this article as: D.M. Blair et al., The structural stability of lunar lava tubes, Icarus (2016), http://dx.doi.org/10.1016/j.icarus.2016.10.008

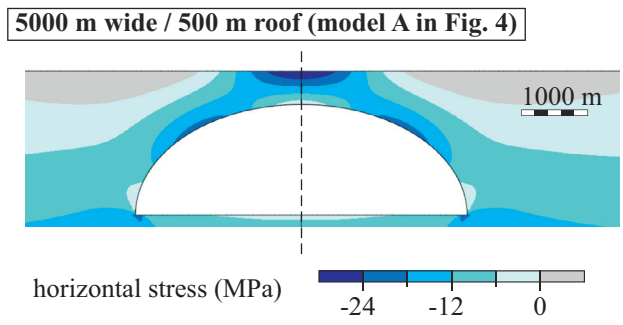

Fig. 4. The largest lava tube found to be theoretically stable, indicated as model A in Fig. 3. The lava tube is 5 km wide, has a roof 500 m thick, and begins in a lithostatic stress state. Color contours show the horizontal stress component with negative (compressional) stresses throughout the roof of the tube.

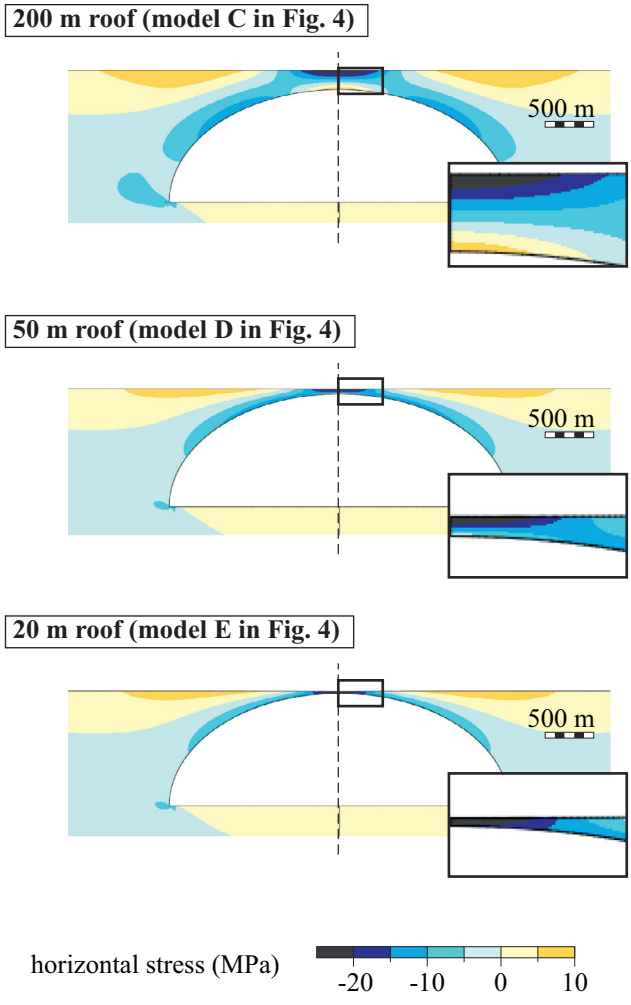

Fig. 5. Models of a 3500 m wide tube with an initial Poisson stress state, showing how varying roof thickness results in different final stress states, failure modes, and stability outcomes. The model with a 200 m roof (model C here and in Fig. 3) fails in extension at the apex of the tube; with a 50 m roof (model D) is stable and shows uniformly compressional horizontal stresses; and with a 20 m roof (model E) fails in compression from the surface downwards. Color contours show the horizontal stress in the model, with positive stress corresponding to tension. Inset boxes show the central portion of the roof magnified for clarity, and the vertical dashed lines represent the plane of symmetry. Shown to scale.

extension (up to +0.03%) combined with a strongly ($\lesssim -20$ MPa) compressional stress state in the roof due to gravity actually serves to bring the lava tube's roof back towards a more neutral stress state, such that several models (B and E) showed an ability to remain stable under more extensional strain than contractional. Models A, B, D, and E (see Fig. 6) also show a rough inverse proportionality between the thickness of a lava tube's roof and the amount of strain that it is able to withstand before failing. Those models which before failed via downwards flexure of the roof (e.g. model C in Fig. 6), however, are far more susceptible to failing when extensional far-field strains are superimposed as opposed to contractional strains, as the addition of still more extensional strain to the system causes the lava tube's roof to sag even farther and quickly leads to pervasive failure at the base of the roof.

4. Discussion

Our results show that lava tubes up to 5 km wide can remain stable under lunar gravity, which is a much larger width than previously expected. Even the smaller stable tubes in our results, such as the 1.5 km wide tube with a 5 m thick roof, which is possible in both the lithostatic and Poisson stress state cases, are several times larger than the 385–500 m stable size calculated by Oberbeck et al. (1969). This is due to the simplification in that analysis where lava tubes are approximated as having a flat roof which acts as a beam, whereas we find that beam-like extensional stresses only occur in the thicker-roofed Poisson-stress-state models (above the dashed line in Fig. 3b). Oberbeck et al. (1969) hypothesized that arched roofs would allow thinner roofs for a given size of lava tube or a larger tube width for the same roof thickness. Our models confirm this hypothesis by showing that with an arched roof lava tubes are more likely to fail in compression rather than tension, which takes advantage of the rock's much higher strength in compression and enables larger lava tubes to remain stable compared to Oberbeck et al. (1969). The fact that an arched roof can allow wider roof spans in masonry structures has been well known since antiquity, so this general result is not in itself surprising.

What may be surprising, however, is the tremendous size (up to 5 km wide) of the largest stable lava tubes in this study, or how thin a roof may be possible while still supporting lava tubes more than a kilometer across. These structures are indeed very large—the lunar horizon lies ~2.4 km away, so in many of the stable tubes modeled here one side of the lava tube's floor would not be visible from the opposing side. For comparison, the largest terrestrial lava tubes are ~30 m in width (e.g. Greeley, 1971), although cave or tunnel chambers formed by other means (such as erosion by subterranean rivers) have been found with widths of several hundred meters (e.g. Ford and Williams, 1994). The larger stable sizes of lava tubes on the Moon can be explained partly by the lower gravity (1/6 that of Earth), which will lead to proportionally lower stresses in the roof in cases where the entire roof is driven into compression by gravity; a cavern 200 m across on Earth could potentially survive at 1200 m across on the Moon for this reason alone assuming linear scaling with overburden pressure. Gravity is only a contributing factor, however, as we find caverns much larger than 1200 m to be stable in these cases. Furthermore, lava tubes which fail due to downwards flexure of the roof which might be expected to follow scaling more like the $g^{1/2}$ factor given by beam theory such that a 200 m terrestrial cavern would correspond to a ~490 m lunar one (closely in line with the value given in Oberbeck et al. (1969)), whereas we find that lava tubes ~2–7 times larger are possible even under flexure, again indicating scaling in excess of that explainable by gravity. Another contributing factor to increased lava tube stability on the Moon may be the almost total lack of aqueous erosion and the assumed "blocky" texture of lunar rocks (i.e. having widely-spaced fractures), which may lead lunar

Please cite this article as: D.M. Blair et al., The structural stability of lunar lava tubes, Icarus (2016), http://dx.doi.org/10.1016/j.icarus.2016.10.008

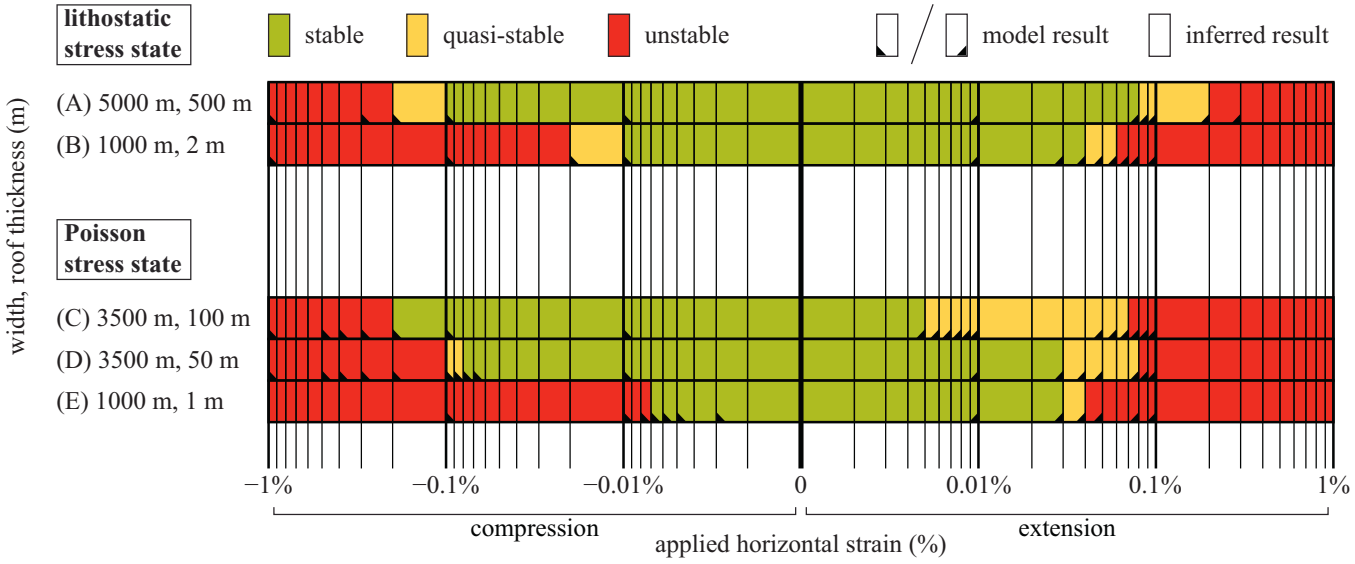

Fig. 6. Stability of various models subjected to far-field tectonic strains. Models are lettered A–E to correspond to those in Figs. 3–5. The amount of contractional or extensional strain is noted on the horizontal axis, with the column of boxes next to 0% strain representing ±0.001%, the next column out representing ±0.002%, and so on. Triangles in the corner of boxes indicate a performed simulation, with results for intermediate amounts of strain inferred from these simulations. Colors and failure states for each model are as in Fig. 3 and explained in the text.

basalts to be stronger (higher cohesion and internal friction angles) than their terrestrial counterparts (after Marinos and Hoek, 2000). In thinner roofs it is also more likely that our continuum assumption is incorrect due to pre-existing fractures in the lava tube's roof. Altering our material parameters to more Earth-like values or changing our continuum approach would thus likely reduce our resulting lava tube sizes, possibly bringing them closer to the size expected from pure gravitational scaling.

Our results also raise the question of whether lava tubes larger than a kilometer across are likely to form under lunar conditions. Although the mechanics of lava tube formation on the Moon are poorly understood, there are several lines of evidence suggesting that tubes several kilometers across may be able to form under lunar conditions. The first of these is the very large, sinuous mass deficits observable in GRAIL gravity data, which indicate some sort of void under the lunar surface—although not necessarily lava tubes—on the order of one kilometer across (Chappaz et al., 2014a; b; 2016). The size of lunar sinuous rilles is also illustrative: Rima Sharp is ~840 m wide on average, Vallis Schröteri ~4.3 km, and there are numerous other rilles with widths over 1 km (e.g. Hurwitz et al., 2013; Garry and Bleacher, 2011). These rilles are generally interpreted to be volcanic in origin, suggesting very high eruption volumes on the Moon. It is possible that among features this size, those with thinner roofs collapsed to form open channels in the form of the observed sinuous rilles, and others with thicker roofs were stable enough to persist as sublunarean lava tubes. Even the global median sinuous rille width, 480 m (Hurwitz et al., 2013), is an order of magnitude larger than known terrestrial examples. This disproportionately larger size of lunar sinuous rilles clearly indicates a different volcanic environment on the two bodies, caused by some combination of factors like crustal stress states, material differences, lava production, or cooling rates. Factors such as the lower viscosity and higher density of lunar lavas, the higher eruption rates inferred at the Moon from observed sinuous rilles, or the absence of convective or advective cooling may also allow the formation of much larger lava tubes on the Moon than on Earth (Cruikshank and Wood, 1971) by enabling more voluminous flows, more cohesive roofs, or thicker chilled lava flow margins, respectively. It is worth noting, however, that air-cooled lava tubes cool more slowly than might be expected due to the insulating effect of gases (Sakimoto and Zuber, 1998), so a radiation-only environment inside a lava tube may not cool at a meaningfully different rate; this question requires further investigation.

The cooling process of a lava tube in an environment such as a lunar mare is also poorly understood, and may have other effects on the stress state and long-term stability of the tube. Cooling of lava during the initial formation process likely does not lead to the development of stresses in the structure, as these will instead be accommodated by pervasive cracking. These cracks will then fill in with subsequent flows, altering the structural properties of the rock as a whole in complex ways. While we attempt to simulate the pervasive weakening through our use of the Geological Strength Index (Marinos and Hoek, 2000), it is possible that subsequent flows may also lead to further cycles of heating and cooling of in-place material, which are not modeled here. These thermal effects would depend on the exact volcanic history of a lava tube, the thicknesses and temperatures of subsequent flows, and, as mentioned above, the specifics of the cooling environment. While this is an admittedly complex parameter space, and is outside the scope of the present study, the complete formation-to-present thermal history of lava tubes does likely play a role in their long-term stability.

Lava tubes ~100–150 m tall (300–450 m wide) that could potentially underlie observed skylights are found to be stable in our calculations even with the very thin (~1 m) roof layer thicknesses observed in the skylights. With both the lithostatic and Poisson initial stress states, there are also models several times larger than this which we find to be stable, so we might not expect structures of these proportions to be particularly "close" to failure; in other words, changes of a factor of two or more in roof thickness or tube width would not affect their stability. This may indicate that, if the skylights are in fact openings into lava tubes, they represent some sort of local failure of otherwise stable structures and not gravitational collapse of fundamentally unstable structures. Meteorite impacts, local concentration of pre-existing fractures, regionally thinner roofs or roof layers, or local material differences could all lead to the formation of skylight-like collapses. Different mechanisms for the formation of the lunar skylights may also be distinguishable by the observed shape of the hole, with irregularly shaped holes representing structural failure instead of an impact

Please cite this article as: D.M. Blair et al., The structural stability of lunar lava tubes, Icarus (2016), http://dx.doi.org/10.1016/j.icarus.2016.10.008

origin (e.g. Martellato et al., 2013). It is worth noting, however, that a skylight could easily form due to a combination of factors, with a nearby meteorite impact triggering the collapse of an already anomalously weak part of the tube or a small but non-penetrating impact creating a weak area which later fails for some other reason. The relative influence of these processes likely varies between individual skylights.

Regional tectonics may also play a role in the location of stable lava tubes. Our results show that lava tubes near the maximum stable size are able to withstand far-field strains between −0.2% and +0.08%, depending on the initial stress state, lava tube size, and roof thickness (see Fig. 6). The presence of any nearby tectonic features (e.g. mare ridges, graben) should thus be carefully considered when attempting to locate or characterize potential lava tubes, as large amounts of regional strain will lead to smaller local maximum lava tube sizes and/or thicker minimum roof thickness than in less tectonically active regions.

Due to their higher gravity, we would expect that similar lava tubes on either Mars or Mercury (both with surface gravity g of $\sim 3.7\ \mathrm{N\,kg^{-1}}$) may be able to remain stable at sizes ∼44% as large as presented here ($\lesssim 2.2$ km wide), or for terrestrial lava tubes ($g \sim 9.8\ \mathrm{N\,kg^{-1}}$) to be able to remain stable when they are ∼16% as large ($\lesssim 800$ m wide), since gravity has a linear effect on the stresses experienced at depth due to overburden. The size of stable lava tubes on a given body would be further reduced by weakening the material comprising the tube either by weathering or the more rapid advective cooling possible in the Martian or terrestrial atmospheres. It is also possible that lava tube aspect ratios other than the 3:1 width-to-height ratio used here could produce different results for stability, and that this ratio may differ between bodies. The exact ways in which lava tube stability is affected by these various factors remains to be investigated. It is important to note, however, that calculations such as those in the present study only represent the sizes at which lava tubes may remain structurally stable; lava tubes 800 m wide are not found on Earth, and so it is entirely possible that lava tubes do not exist at these maximum sizes on the Moon, Mars, or Mercury. The maximum size of extant (as opposed to structurally possible) lava tubes may thus be controlled more by the properties of the source of the tube-forming lava flow than by the stability of the formed lava tube.

5. Conclusions

We use finite element models to test the stability of lava tubes of various sizes and burial depths under a variety of conditions appropriate to the lunar maria. By calculating material failure in the lava tubes' roofs, we conclude that large (kilometer scale) vacant sublunarean lava tubes may be able to remain stable on the Moon under a wide range of possible conditions. Our results suggest that a lava tube ∼5 km wide can remain stable given that it formed in sufficiently voluminous lava flows that it possesses a thick (500 m) roof, and given a near-lithostatic initial stress state and a comparatively quiescent regional tectonic environment. Lava tubes ∼1 km wide may be able to remain stable with a roof only ∼2 m thick, given similar initial and regional stress conditions. Both of these results assume a set of Geological Strength Index parameters and a rock density appropriate to the lunar maria, an unconfined compressive strength of 100 MPa, and a lava tube with an assumed 3:1 width-to-height ratio. These results indicate that the interpretation of Chappaz et al. (2014a,b, 2016) that GRAIL data suggests the presence of several-kilometer-wide voids buried beneath the lunar surface is within the realm of mechanical plausibility.

The primary factor which allows large lava tubes to remain stable is the arched shape of the roof, which leads to a compressional stress state throughout the roof under gravitational loading. This result, when scaled for gravity, leads to stable lava tube sizes on Earth much larger than known examples. The size of the largest extant vacant lava tube on a given body may thus be limited not by stability issues, but by the manner and scale of their formation or by erosional processes that decrease the durability of larger tubes. Therefore, while both this study and gravitational evidence from GRAIL (Chappaz et al., 2014a,b, 2016) support the possibility that lava tubes several kilometers across may exist under the lunar surface, further proof of their existence gathered by methods such as ground-penetrating RADAR (e.g. Sood et al., 2016c), gravimetry (e.g. Urbancic et al., 2015) or seismic studies will be needed before their existence can be confirmed.

Acknowledgements

We would like to thank Dr. Junichi Haruyama of the Japan Aerospace Exploration Agency (JAXA), Dr. Tracy Gregg of the University of Buffalo, and Dr. Debra Hurwitz of the Lunar and Planetary Institute for their insightful and helpful comments. This work was supported by NASA Headquarters under the NASA Earth and Space Science Fellowship Program, grant NNX13AO63H. It has also been supported by the GRAIL mission, which is part of NASA's Discovery Program performed under contract to the Massachusetts Institute of Technology and the Jet Propulsion Laboratory.

References

Ashley, J.W., Boyd, A.K., Hiesinger, H., Robinson, M.S., Tran, T., van der Bogert, C.H., Wagner, R.V.and the LROC Science Team, 2011. Lunar pits: sublunarean voids and the nature of mare emplacement. Lunar Planet. Sci. Conf. 42 abstract 2771.

Ashley, J.W., Robinson, M.S., Hawke, B.R., van der Bogert, C.H., Hiesinger, H., Sato, H., Speyerer, E.J., Enns, A.C., Wagner, R.V., Young, K.E., Burns, K.N., 2012. Geology of the king crater region: new insights into impact melt dynamics on the Moon. J. Geophys. Res. 117, E00H29. doi:10.1029/2011JE003990.

Chappaz, L., Melosh, H.J., Howell, K.C.and the GRAIL mission team, 2014a. Surface and buried lava tube detection with GRAIL data. Lunar Planet. Sci. Conf. 45 abstract 1746.

Chappaz, L., Sood, R., Melosh, H., Howell, K., 2014b. Buried empty lava tube detection with GRAIL data. American Inst. Aeronautics Astronautics SPACE 2014 Conf. and Expo. abstract 4371 doi:10.2514/6.2014-4371.

Chappaz, L., Sood, R., Melosh, H.J., Howell, K.C., Blair, D.M., Milbury, C., Zuber, M.T., (2016), Evidence of large empty lava tubes on the moon using GRAIL gravity, in prep.

Coombs, C.R., Hawke, B.R., 1992. A search for intact lava tubes on the Moon: possible lunar base habitats. In: Mendell, W.W. (Ed.), *The Second Conference on Lunar Bases and Space Activities of the 21st Century, NASA Conferences Publication*, 3166 1, pp. 219–229. (Parts 1–4) & *2* (Parts 5–8).

Cruikshank, D.P., Wood, C.A., 1971. Lunar rilles and Hawaiian volcanic features: possible analogues. The Moon 3, 412–447. doi:10.1007/BF00562463.

Ford, D., Williams, P., 1994. Karst Geomorphology and Hydrology. Chapman & Hall, London, UK, pp. 309–315. doi:10.1002/9781118684986.

Garry, W.B., Bleacher, J.E., 2011. Emplacement scenarios for Vallis Schröteri, Aristarchus plateau. In: Ambrose, W.A., Williams, D.A. (Eds.). In: Recent Advances and Current Research Issues in Lunar Stratigraphy, Special Paper, 477. Geological Society of America, pp. 77–93. doi:10.1130/2011.2477(03).

Greeley, R., 1971. Lava tubes and channels in the lunar Marius hills. The Moon 3, 289–314. doi:10.1007/BF00561842.

Haruyama, J., Hioki, K., Shirao, M., Morota, T., Hiesinger, H., van der Bogert, C.H., Miyamoto, H., Iwasaki, A., Yokota, Y., Ohtake, M., Matsunaga, T., Hara, S., Nakanotani, S., Pieters, C.M., 2009. Possible lunar lava tube skylight observed by SELENE cameras. Geophys. Res. Lett. 36, L21206. doi:10.1029/2009GL040635.

Haruyama, J., Hara, S., Hioki, K., Morota, T., Yokota, Y., Shirao, M., Hiesinger, H., van der Bogert, C.H., Miyamoto, H., Iwasaki, A., Ohtake, M., Saito, Y., Matsunaga, T., Nakanotani, S., Pieters, C.M., Lucey, P.G., 2010. New discoveries of lunar holes in mare tranquilltatis and mare ingenii. Lunar Planet. Sci. Conf. 41 abstract 1285.

Haruyama, J., Morota, T., Kobayashi, S., Sawai, S., Lucey, P.G., Shirao, M., Nishino, M.N., 2012. Lunar holes and lava tubes as resources for lunar science and exploration. In: Badescu, V. (Ed.), Moon: Prospective Energy and Material Resources. Springer, Heidelberg, Germany, pp. 139–163. doi:10.1007/978-3-642-27969-0.

Hörz, F., 1985. Lava tubes: potential shelters for habitats. In: Mendell, W.W. (Ed.), Lunar Bases and Space Activities of the 21st Century (A86-30113 13-14). Lunar and Planetary Institute, Houston, TX, pp. 405–412. doi:10.1016/0016-7037(87)90018-4.

Hurwitz, D.M., Head, J.W., Hiesinger, H., 2013. Lunar sinuous rilles: distribution, characteristics, and implications for their origin. Planet. Space Sci. 79-80, 1–38. doi:10.1016/j.pss.2012.10.019.

Kiefer, W.S., Macke, R.J., Britt, D.T., Irving, A.J., Consolmagno, G.J., 2012. The density and porosity of lunar rocks. Geophys. Res. Lett. 39, L07201. doi:10.1029/2012GL051319.

Lemoine, F.G., Goossens, S., Sabaka, T.J., Nicholas, J.B., Mazarico, E., Row- lands, D.D., Loomis, B.D., Chinn, D.S., Neumann, G.A., Smith, D.E., Zuber, M.T., 2014. GRGM900c: a degree 900 lunar gravity model from GRAIL primary and extended mission data. Geophys. Res. Lett. 41 (10), 3382–3389.

Marinos, P., Hoek, E., 2000. GSI: a geologically friendly tool for rock mass strength estimation. In: Proc. GeoEng2000 Conf. Melbourne. Australia, pp. 1422–1442.

Martellato, E., Foing, B.H., Benkhoff, J., 2013. Numerical modelling of impact crater formation associated with isolated lunar skylight candidates on lava tubes. Planet. Space Sci. 86, 33–44. doi:10.1016/j.pss.2013.06.010.

Oberbeck, V.R., Quaide, W.L., Greeley, R., 1969. On the origin of lunar sinuous rilles. Modern Geol 1, 75–80.

Oberbeck, V.R., Aoyagi, M., Greeley, R., Lovas, M., 1972. Planimetric shapes of lunar rilles. Apollo 16 Preliminary Science Report, Part Q. pp. 29–80 to 29–88, NASA SP-315.

Palmer, A.N., 2007. In: Watson, R.A. (Ed.), Cave Geology. Cave Books, Dayton, OH, pp. 161–163.

Robinson, M.S., Brylow, S.M., Tschimmel, M., Humm, D., Lawrence, S.J., Thomas, P.C., Denevi, B.W., Bowman-Cisneros, E., Zerr, J., Ravine, M.A., Caplinger, M.A., Ghaemi, F.T., Schaffner, J.A., Malin, M.C., Mahanti, P., Bartels, A., Anderson, J., Tran, T.N., Eliason, E.M., McEwen, A.S., Turtle, E., Jolliff, B.L., Hiesinger, H., 2010. Lunar reconnaissance orbiter camera (LROC) instrument overview. Space Sci. Rev. 150 (1–4), 81–124. doi:10.1007/s11214-010-9634-2.

Robinson, M.S., Ashley, J.W., Boyd, A.K., Wagner, R.V., Speyerer, E.J., Ray Hawke, B., Hiesinger, H., van der Bogert, C.H., 2012. Confirmation of sublunarean voids and thin layering in mare deposits. Planet. Space Sci. 69, 18–27. doi:10.1016/j.pss.2012.05.008.

Sakimoto, S.E.H., Zuber, M.T., 1998. Flow and convective cooling in lava tubes. J. Geophys. Res. 103 (B11), 27465–27487.

Sood, R., Chappaz, L., Melosh, H.J., Howell, K.C., Milbury, C., 2016a. Detection of buried empty lunar lava tubes using GRAIL gravity data. Lunar Planet. Sci. Conf. 47 abstract 1509.

Sood, R., Chappaz, L., Melosh, H.J., Howell, K.C., Milbury, C., Blair, D.M., Zuber, M.T., 2016b. Detection and characterization of buried lunar craters with GRAIL data, submitted.

Sood, R., Melosh, J., Howell, K., 2016c. Lunar advanced radar orbiter for subsurface sounding (LAROSS): lava tube exploration mission. AAS/AIAA 26th Space Flight Mechanics Meeting.

Urbancic, N., Stanley, S., Ghent, R., Carroll, K.A., Hatch, D., Williamson, M.C., Garry, W.B., Talwani, M., 2015. Exploring lunar sub-surface objects using surface gravimetric surveys. Lunar. Planet. Sci. Conf. 46 abstract 1616.

Wagner, R.V., Robinson, M.S., 2014. Distribution, formation mechanisms, and significance of lunar pits. ICARUS 237, 52–60. doi:10.1016/j.icarus.2014.04.002.

Wieder, S.Z., Crawford, I.A., Joy, K.H., 2010. Individual lava flow thicknesses in oceanus procellarum and mare serenitatis determined from clementine multispectral data. ICARUS 209, 323–336. doi:10.1016/j.icarus.2010.05.010.

Zuber, M.T., Smith, D.E., Watkins, M.M., Asmar, S.W., Konopliv, A.S., Lemoine, F.G., Melosh, H.J., Neumann, G.A., Phillps, R.J., Solomon, S.C., Wieczorek, M.A., Williams, J.G., Goossens, S.J., Kruizinga, G., Mazarico, E., Park, R.S., Yuan, D.-H., 2013. Gravity field of the Moon from the gravity recovery and interior laboratory (GRAIL) mission. Science 339, 668–671. doi:10.1126/science.1231507.

Please cite this article as: D.M. Blair et al., The structural stability of lunar lava tubes, Icarus (2016), http://dx.doi.org/10.1016/j.icarus.2016.10.008